Unsteady Natural Convection in a Square Cavity Partially Filled with Porous Media Using a Thermal Non-Equilibrium Model

Ammar Alsabery, Habibis Saleh, Norazam Arbin, Ishak Hashim

Abstract—Unsteady natural convection and heat transfer in a square cavity partially filled with porous media using a thermal non-equilibrium model is studied in this paper. The left vertical wall is maintained at a constant hot temperature T_h and the right vertical wall is maintained at a constant cold temperature T_c, while the horizontal walls are adiabatic. The governing equations are obtained by applying the Darcy model and Boussinesq approximation. COMSOL's finite element method is used to solve the non-dimensional governing equations together with specified boundary conditions. The governing parameters of this study are the Rayleigh number ($Ra = 10^5$, and $Ra = 10^6$), Darcy number ($Da = 10^{-2}$, and $Da = 10^{-3}$), the modified thermal conductivity ratio ($10^{-1} \leq \gamma \leq 10^4$), the inter-phase heat transfer coefficien ($10^{-1} \leq H \leq 10^3$) and the time dependent ($0.001 \leq \tau \leq 0.2$). The results presented for values of the governing parameters in terms of streamlines in both fluid/porous-layer, isotherms of fluid in fluid/porous-layer, isotherms of solid in porous layer, and average Nusselt number.

Keywords—Unsteady natural convection, Thermal non-equilibrium model, Darcy model.

I. Introduction

NATURAL convection fluid flow and heat transfer in porous media domains has received considerable attention over the past few years and the importance of this issue is back to the wide range of environmental situations or industrial applications, such as, geothermal systems, thermal insulation, filtration processes, ground water pollution, storage of nuclear waste, drying processes, solidification of castings, storage of liquefied gases, biofilm growth, fuel cells. The problem dealing with the fluid motions in the clear region and the porous medium has been studied for many years. Reference [1] presented the simple situation of the boundary conditions between a porous media and a homogeneous fluid. Meanwhile, [2] studied natural convection flow and heat transfer between a fluid layer and a porous layer inside a rectangular enclosure. Natural convection heat and mass transfer in solidification was studied by [3]. On the other hand, [4] investigated the convective stability in a superposed fluid and porous layer when heated from below, heat transfer and fluid flow through fibrous insulation presented by [5]. The problem with studying the solute exchange by convection within estuarine sediments has been considered by [6]. Reference [7] discussed the problem of using one- or two domain formulations for the

conservation equations. Meanwhile, [8] studied the particular subclass of such problems where natural convection takes place in a confined enclosure partially filled with a porous medium.

Most of the previous studies considered the natural convection fluid flow and heat transfer in porous media domains in local thermodynamic equilibrium where the fluid temperature is equal to the solid temperature in partially porous media. While, in case where the fluid temperature is different to the solid temperature, we call this as the local thermal non-equilibrium model. Many studies have considered the thermal equilibrium model in partially porous medium, while the non-equilibrium model has not received much attention. Reference [9] have considered the modelling of heat transfer by conduction in a transition region between a porous medium and an external fluid. Reference [10] applied the heat transfer conditions at the boundary between a porous medium and a homogeneous fluid. Their study showed that the jump parameters take the form of the boundary conditions involving surface excess quantities. Reference [11] used the concept of local thermal equilibrium model on free convection in open-ended vertical channels partially filled with porous material. Reference [12] analytically studied the two-step up-scaling approach to determine the jump relations that must be imposed at the interface between a homogeneous porous domain and a free domain under the assumption of local thermal equilibrium.

On the other hand, little work has been done on the local thermal non-equilibrium model in partially porous medium. Reference [13] investigated the effect of using the local thermal non-equilibrium model on forced convection heat transfer flows in a tube filled with a fluid-saturated porous medium. Reference [14] studied numerically the effects using local thermal non-equilibrium model on steady and unsteady natural convection and heat transfer in a channel partially filled with porous media. A recent problem considered different number of equations: a two-temperature model and a one-temperature model at a fluid-porous interface using local thermal non-equilibrium model was studied by [15]. However, there is not much work have been done on natural convection fluid flow and heat transfer in porous media using local thermal non-equilibrium model.

The aim of this study is to investigate the effect of unsteady Darcy model on natural convection and heat transfer in a square cavity partially filled with porous media using a thermal non-equilibrium model.

A. Alsabery (Corresponding author), H. Saleh and N. Arbin are with the School of Mathematical Sciences, Universiti Kebangsaan Malaysia, 43600 Bangi Selangor, Malaysia e-mail: (see ammar_e_2011@yahoo.com).
I. Hashim is with the Solar Energy Research Institute, Universiti Kebangsaan Malaysia, 43600 UKM Bangi Selangor, Malaysia.

II. Mathematical Formulation

Consider the unsteady, two-dimensional natural convection flow and heat transfer in a square cavity partially filled with porous media as shown in Fig. 1. It is assumed that the left vertical wall of the cavity is maintained at a constant hot temperature T_h and the right vertical wall is maintained at a constant cold temperature T_c, while the horizontal walls are adiabatic. A square cavity with horizontal range of the fluid layer denoted by length S, while the total dimensions of the square cavity is L. The fluid and the solid matrix have different temperatures by assuming the convective fluid and the porous medium are not in a local thermodynamic equilibrium. According to the Boussinesq approximation, the fluid physical properties are constant except for the density. By considering these assumptions, the conservation equations for mass, Darcy and energy equations for unsteady natural convection for the fluid and the porous layer will be considered separately. For the fluid layer we have:

$$\frac{\partial u_f}{\partial x} + \frac{\partial v_f}{\partial y} = 0, \tag{1}$$

$$\frac{\partial u_f}{\partial t} + u_f \frac{\partial u_f}{\partial x} + v_f \frac{\partial u_f}{\partial y} = -\frac{1}{\rho_f} \frac{\partial p_f}{\partial x}$$
$$+ \nu \left(\frac{\partial^2 u_f}{\partial x^2} + \frac{\partial^2 u_f}{\partial y^2} \right), \tag{2}$$

$$\frac{\partial v_f}{\partial t} + u_f \frac{\partial v_f}{\partial x} + v_f \frac{\partial v_f}{\partial y} = -\frac{1}{\rho_f} \frac{\partial p_f}{\partial x}$$
$$+ \nu \left(\frac{\partial^2 v_f}{\partial x^2} + \frac{\partial^2 v_f}{\partial y^2} \right) + \rho g \beta \left(T_f - T_c \right), \tag{3}$$

$$\frac{\partial T_f}{\partial t} + u_f \frac{\partial T_f}{\partial x} + v_f \frac{\partial T_f}{\partial y} = \left(\frac{\partial^2 T_f}{\partial x^2} + \frac{\partial^2 T_f}{\partial y^2} \right)$$
$$+ \frac{K_f}{\rho_f C_f} \left(T_f - T_p \right), \tag{4}$$

The conservation equations for mass, Darcy and energy equations for the homogenous porous layer are:

$$\frac{\partial u_p}{\partial x} + \frac{\partial v_p}{\partial y} = 0, \tag{5}$$

$$u_p = -\frac{K_p}{\mu} \frac{\partial p_p}{\partial x}, \tag{6}$$

$$v_p = -\frac{K_p}{\mu} \frac{\partial p_p}{\partial x} + \frac{K_p \beta g}{\nu} \left(T_p - T_c \right), \tag{7}$$

$$\varphi_p \left(\rho C_p \right)_p + \left(\rho C_p \right)_p \left(u_p \frac{\partial T_p}{\partial x} + v_p \frac{\partial T_p}{\partial y} \right) = \varphi k_p$$
$$\times \left(\frac{\partial^2 T_p}{\partial x^2} + \frac{\partial^2 T_p}{\partial y^2} \right) + \frac{\mu_p}{(\rho C_p)_p} \left(u_p^2 + v_p^2 \right)$$
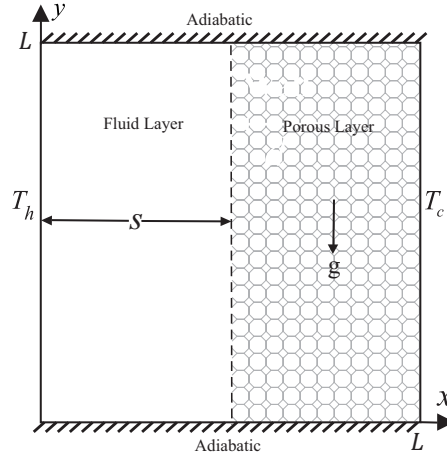$$+ h \left(T_s - T_p \right), \tag{8}$$

Fig. 1. Physical model with coordinate system of convection in a square porous cavity

$$(1 - \varphi_p) \left(\rho C_p \right)_s \frac{\partial T_s}{\partial t} + (1 - \varphi_p) k_s \left(\frac{\partial^2 T_s}{\partial x^2} + \frac{\partial^2 T_s}{\partial y^2} \right)$$
$$= h \left(T_s - T_p \right). \tag{9}$$

where x and y are the cartesian coordinates measured in the horizontal and vertical directions respectively, u_f, u_p, v_f and v_p are the velocity components in the x and y directions for the fluid and porous layers respectively, K_p is the permeability of the porous medium and g is the acceleration due to gravity.

The values of the velocities are zero on the walls. The boundary conditions for both the fluid and the porous layer at interface are:

$$T \mid_{x=s^-} = T \mid_{x=s^+}, \tag{10}$$

$$U \mid_{x=s^-} = U_p \mid_{x=s^+}, \quad V \mid_{x=s^-} = V_p \mid_{x=s^+}. \tag{11}$$

In terms of the stream function ψ defined in the usual way as $u = \partial \psi / \partial y$ and $v = -\partial \psi / \partial x$ together with the following non-dimensional variables:

$$\Psi = \frac{\psi}{\alpha_m \varphi L}, \quad \theta_p = \frac{T_p - T_c}{T_h - T_c},$$

$$\theta_s = \frac{T_s - T_c}{T_h - T_c}, \quad \theta_f = \frac{T_f - T_c}{T_h - T_c},$$

$$t = \frac{\alpha_m}{L^2} t', \quad X = \frac{x}{L}, \quad Y = \frac{y}{L}. \tag{12}$$

The governing equations for the fluid layer can be written as:

$$U_f \frac{\partial U_f}{\partial X} + V_f \frac{\partial U_f}{\partial Y} = -\frac{\partial P_f}{\partial X} + \left(\frac{\partial^2 U_f}{\partial X^2} + \frac{\partial^2 U_f}{\partial Y^2} \right), \tag{13}$$

$$U_f \frac{\partial V_f}{\partial X} + V_f \frac{\partial V_f}{\partial Y} = -\frac{\partial P_f}{\partial Y} + \left(\frac{\partial^2 V_f}{\partial X^2} + \frac{\partial^2 V_f}{\partial Y^2} \right) + \frac{Ra}{Pr}\theta, \quad (14)$$

$$U_f \frac{\partial \theta_f}{\partial X} + V_f \frac{\partial \theta_f}{\partial Y} = \frac{1}{Pr} \left(\frac{\partial^2 \theta_f}{\partial X^2} + \frac{\partial^2 \theta_f}{\partial Y^2} \right), \quad (15)$$

The governing equations for the porous layer can be written as:

$$\frac{\partial^2 \Psi_p}{\partial X^2} + \frac{\partial^2 \Psi_p}{\partial Y^2} = -Ra \frac{\partial \theta_p}{\partial X}, \quad (16)$$

$$\frac{\partial \theta_p}{\partial t} + \frac{\partial \Psi_p}{\partial Y} \frac{\partial \theta_p}{\partial X} - \frac{\partial \Psi}{\partial X} \frac{\partial \theta_p}{\partial Y} = \frac{\partial^2 \theta_p}{\partial X^2}$$
$$+ \frac{\partial^2 \theta_p}{\partial Y^2} + H_p \left(\theta_s - \theta_p \right), \quad (17)$$

$$\frac{\partial \theta_s}{\partial t} = \frac{1}{\Gamma_p} \left(\frac{\partial^2 \theta_s}{\partial X^2} + \frac{\partial^2 \theta_s}{\partial Y^2} \right) + \gamma_p H_p \left(\theta_s - \theta_p \right), \quad (18)$$

where the parameters H, γ and Γ are defined as:

$$H = \frac{hL^2}{\varphi k_p}, \quad \gamma = \frac{\varphi k_p}{(1-\varphi) k_s}, \quad \Gamma = \frac{\alpha_p}{\alpha_s}, \quad (19)$$

and α_p and α_s are the thermal diffusivities of the fluid and solid phases in porous layer, respectively, $Ra = g\beta(T_h - T_c)L^3/(\alpha_f \nu_f)$ is the Rayleigh number for both the fluid and the porous layer, $Pr = \nu_f/\alpha_f$ is the Prandtl number for the fluid layer.

The dimensionless boundary conditions of (16)–(15) are:

$$\Psi = 0, \quad \theta_p = \theta_s = 1, \quad \text{at} \quad X = 0,$$

$$\Psi = 0, \quad \theta_p = \theta_s = 0, \quad \text{at} \quad X = 1,$$

$$\Psi = 0, \quad \frac{\partial \theta_f}{\partial Y} = \frac{\partial \theta_s}{\partial Y} = 0, \quad \text{at} \quad Y = 0, 1, \quad (20)$$

and at the interface by using the matching conditions proposed by [1]

$$\theta \mid_{X=s^-} = \theta \mid_{X=s^+}, \frac{\partial u}{\partial X} = \overline{\alpha}(u^- - v^+)/\sqrt{Da}, \quad (21)$$

$$kf\frac{\partial T}{\partial X}s^- = kp\frac{\partial T}{\partial X}s^+. \quad (22)$$

where in our study the value of $\overline{\alpha}$ fix at 1.
The local Nusselt number:

$$Nu\left(Y\right) = - \left(\frac{\partial \theta_{p,s}}{\partial X} \right)_{X=0,1}. \quad (23)$$

S	present result	[16]	[17]
0.25	3.103	3.083	3.101
0.50	3.350	3.321	3.348
0.75	3.605	3.600	3.604

Finally, the average Nusselt number at the left vertical wall for the fluid and solid phases in porous layer are given by:

$$\overline{Nu}_p = \int_0^1 Nu\left(Y\right) dX, \quad (24)$$

$$\overline{Nu}_s = \int_0^1 Nu\left(Y\right) dX. \quad (25)$$

III. NUMERICAL METHOD AND VALIDATION

Based on the Galerkin finite element method (GFEM), the governing equations subject to the boundary conditions are solved numerically using the CFD software package COMSOL Multiphysics, a general-application solver and simulation of interconnected partial differential equation. This flexible platform contains the art numerical algorithms and visualization tools bundled together with an easy to use interface. The COMSOL's finite element method was applied to solve (16), the momentum equation in fluid layer (13), the heat transfer in fluids equation in porous layer (17), the heat transfer in solids equation in porous layer (18) and the heat transfer in fluids equation in fluid layer (15) subject to the boundary conditions (20).

In this investigation, mesh generation on oblique cavity is made by using graph grid. By considering both of the accuracy and the time, finer, extra fine and extremely fine mesh sizes were selected for all the computations done in this study. As a validation, we compared our results with those presented by [16] and [17] by calculating average Nusselt number with various values of dimensionless fluid layer thickness as shown in Table I. A very good agreement was found between our results and the existing results. To confirm the validity of the results, we compared our figure with what was presented by [18] as shown in Fig. 2. Fig. 2 shows the comparison between present result and result presented by [18] for $Ra = 10^3$, $\gamma = 1$ and $S = 0$.

IV. RESULTS AND DISCUSSION

In this section, we present numerical results for the streamlines of porous layer, streamlines of fluid layer, isotherms of fluid and isotherms of solid porous layer and isotherms of fluid layer for various values of Darcy number (10^{-2} and 10^{-3}), the modified thermal conductivity ratio ($10^{-1} \leq \gamma \leq 10^4$), the inter-phase heat transfer coefficien ($10^{-1} \leq H \leq 10^3$), the time independent ($0.001 \leq \tau \leq 0.2$), Rayleigh number ($Ra = 10^5$ and 10^6) and Prandtl number $Pr = 6.2$. The values of the average Nusselt number have been calculated for various values of γ.
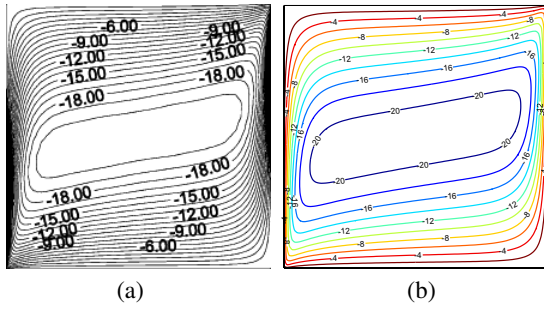
Fig. 2.   Streamlines [18] (a), present study (b) for $Ra = 10^3$, $\gamma = 1$ and $S = 0$

In terms of the streamlines and isotherms of fluid in fluid/porous-layer and isotherms of solid in porous layer, Fig. 3 shows the changes of the flow motion and the distribution of heat transfer for high value of Rayleigh number, $Ra = 10^6$, with different values of the modified thermal conductivity ratio, $\gamma = 0.1, 10, 100$ and 1000. The values of Darcy number, inter-phase heat transfer coefficient, fluid layer thickness and time independent were fixed at 10^{-3}, $H = 1$, $S = 0.5$ and $\tau = 0.1$, respectively. Fig. 3 (a) presents the streamlines of the fluid/porous-layer and the isotherm patterns at low value of the modified thermal conductivity ratio, ($\gamma = 0.1$). The temperature of the left wall is higher than the flow temperature inside the fluid partition, and when the temperature starts to rises, the flow starts to move from the left wall (hot) to the interface and through the interface the flow start to leave the fluid partition and infiltrate in the porous layer to the right wall (cold) and falling along the right wall, then rising again at the hot wall, creating a clockwise rotating cell inside the fluid partition approaching to the interface. The isotherms appear with bend upwards when the flow infiltrate to the porous layer. The streamlines circulate as vortices in clockwise direction (negative sign of Ψ) it will present by $\Psi_{\min}$. The fact that the fluid layer is higher effective thermal conductivity than the porous layer, so most of the temperature drop takes place in the fluid partition. The distortion of the isotherms of solid in the porous layer appears with curved lines to the top. The streamlines inside the fluid partition nearing to the interface as shown in Fig. 3 (b) and c clearly show that the streamlines cell tend to decrease by increasing γ, by increasing γ, the $\Psi_{\min}$ tends to decrease(see $\Psi_{\min}$ values). As the modified thermal conductivity ratio increases, the distortion of the isotherms of solid in the porous layer decreases. By increasing the modified thermal conductivity ratio to ($\gamma = 1000$) the isotherms of solid are almost the same as the isotherms of fluid in the porous layer as shown in Fig. 3 (d).

Fig. 4 shows the unsteady results on the streamlines and isotherms of fluid in the fluid/porous-layer and isotherms of solid in porous layer for $Ra = 10^6$, $Da = 10^{-3}$, $Pr = 6.2$, $\gamma = 10$, $H = 10$ and $S = 0.5$. Early time after the start of heating ($0.005 \leq \tau \leq 0.01$) in the unsteady, the streamlines cell near to hot wall (fluid partition) start to decreases and tends to take the elliptical shape with moving near to the hot wall. The $\Psi_{\min}$ decreases by increasing the time (see $\Psi_{\min}$

(a) $\gamma = 0.1$

(b) $\gamma = 10$

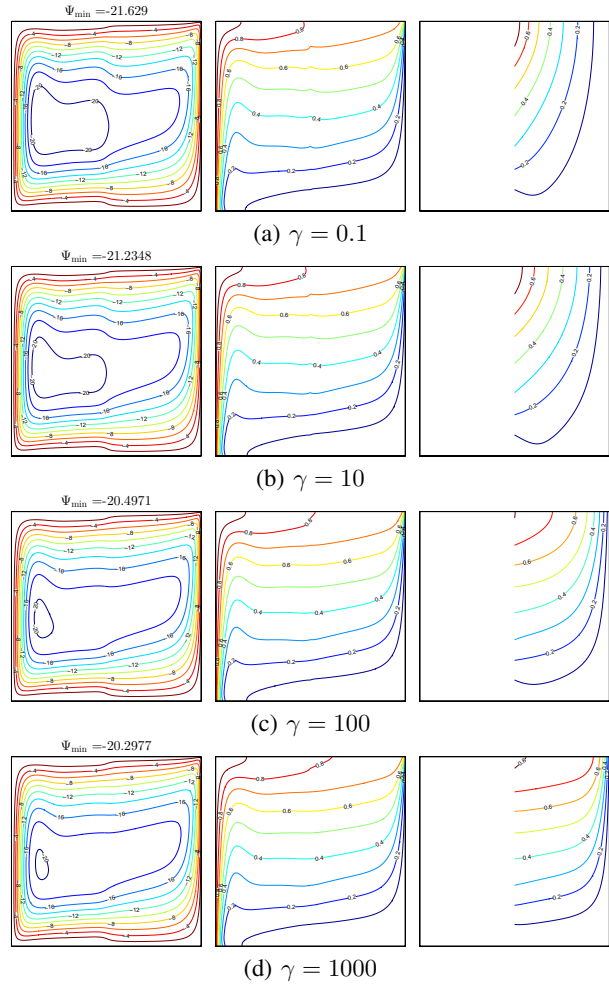(c) $\gamma = 100$

(d) $\gamma = 1000$

Fig. 3.   Unsteady streamlines (left), isotherms for fluid phase (middle) and isotherms for solid phase (right) evolution by modified thermal conductivity ratio for $Ra = 10^6$, $Da = 10^{-3}$, $H = 1$, $S = 0.5$ and $\tau = 0.1$.

vales). After the start of heating, the distortion of the isotherms of fluid in the fluid/porous-layer appears with vertical lines near to the hot wall (fluid partition), near to interface the heat lines tend to become diagonal, while the distortion of the isotherms near to right wall (porous partition) appears with horizontal lines by increasing time. The distortion of the isotherms of solid in the porous layer appears from the top of the interface with diagonal lines. By increasing the time to $\tau = 0.05$ as shown in Fig. 4 (c), the streamlines cell near to the hot wall decreasing constantly. By increasing the time to $\tau = 0.2$ as shown in Fig. 4 (d), the steady state has been reached, the streamline cell near to hot wall disappear. The $\Psi_{\min}$ constantly decreases by increasing the time (see $\Psi_{\min}$ vales).

The variations of the steady average Nusselt number of the fluid (a) and the solid (b) with modified thermal conductivity ratio for different H at $Ra = 10^5$, $Da = 10^{-2}$ and $S = 0.5$ are shown in Fig. 5. Fig. 5 (a) clearly shows that the average Nusselt number of the fluid in the porous layer decreases as
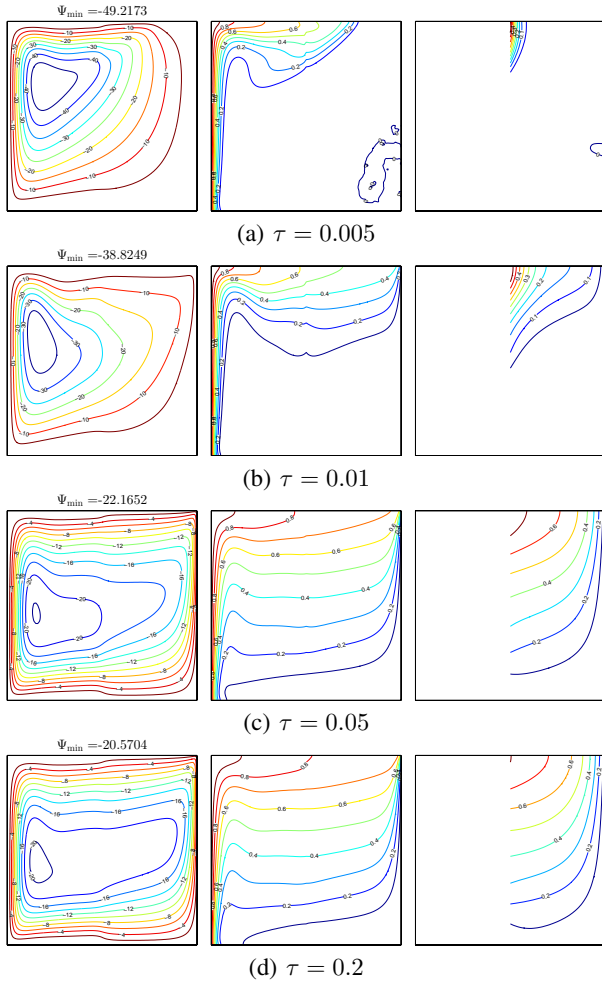
(a) $\tau = 0.005$

(b) $\tau = 0.01$

(c) $\tau = 0.05$

(d) $\tau = 0.2$

Fig. 4. Unsteady streamlines (left), isotherms for fluid phase (middle) and isotherms for solid phase (right) evolution by time for $Ra = 10^6$, $Da = 10^{-3}$, $\gamma = 1$, $H = 1$ and $S = 0.5$.

modified thermal conductivity ratio increases. The significant decreasing of the average Nusselt number occurs for high values of H, ($H = 100, 1000$) by increasing modified thermal conductivity ratio. Fig. 5 (b) clearly shows that the average Nusselt number of the solid in the porous layer decreases as modified thermal conductivity ratio increases. The significant increase of the average Nusselt number occurs for high values of H, ($H = 100, 1000$).

V. CONCLUSION

The present numerical simulation considered the effects of unsteady Darcy model on natural convection and heat transfer in a square cavity partially filled with porous media using a Thermal non-equilibrium model. The COMSOL's finite element method was used to solve the dimensionless form of the governing equations. Detailed computational results for flow, temperature field in both fluid/porous layer in the cavity and the average Nusselt number of the fluid and the solid in the porous layer have been presented in the graphical form.
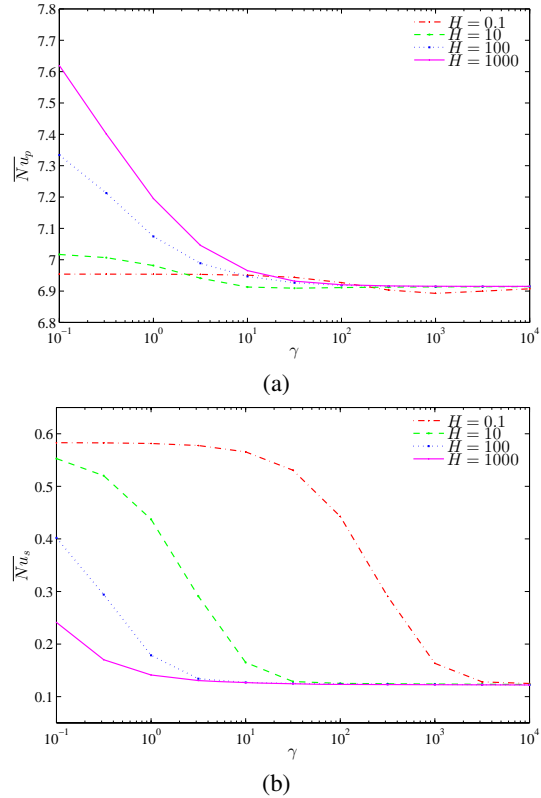

(a)

(b)

Fig. 5. Variation of the steady average Nusselt number of fluid (a) and solid (b) interfaces with γ for different H at $Ra = 10^5$, $Da = 10^{-2}$, and $S = 0.5$.

The main conclusions of the present study are as follows:

1) The unsteady strength of the flow circulation decreases by increasing the modified thermal conductivity ratio. As γ increases, the distortion of the isotherms appear with bend upwards when the flow infiltrate to the porous layer, whereas the distortion of the isotherms of solid in the porous layer increases and becomes almost the same as the isotherms of fluid in the porous layer by increasing the modified thermal conductivity ratio.

2) The unsteady strength of the flow circulation decreases by increasing the time. By increasing the time to $\tau = 0.2$, the steady state has been reached. The distortion of the isotherms of fluid in the porous/fluid-layer increases by increasing the time.

3) The steady average Nusselt number of the fluid in the porous layer decreases as modified thermal conductivity ratio increases. The significant decreasing of the average Nusselt number occurs for high values of H. The steady average Nusselt number of the solid decreases as γ increases. The significant increasing of the average Nusselt number occurs for high values of H.

REFERENCES

[1] G. S. Beavers and D. D. Joseph, "Boundary conditions at a naturally permeable wall," *Journal of fluid mechanics*, 30(01):197–207, 1967.

[2] C. Beckermann, S. Ramadhyani, and R. Viskanta, "Natural convection flow and heat transfer between a fluid layer and a porous layer inside a rectangular enclosure," *Journal of heat transfer*, 109(2):363–370, 1987.

[3] C. Beckermann, R. Viskanta, and S. Ramadhyani, "Natural convection in vertical enclosures containing simultaneously fluid and porous layers," *Journal of Fluid Mechanics*, 186:257–284, 1988.

[4] F. Chen and C. F. Chen, "Experimental investigation of convective stability in a superposed fluid and porous layer when heated from below," *Journal of Fluid Mechanics*, 207:311–321, 1989.

[5] P. L. Breton, J. P. Caltagirone, and E. Arquis, "Natural convection in a square cavity with thin porous layers on its vertical walls," *Journal of heat transfer*, 113(4):892–898, 1991.

[6] I. T. Webster, S. J. Norquay, F. C. Ross, and R. A. Wooding, "Solute exchange by convection within estuarine sediments," *Estuarine, Coastal and Shelf Science*, 42(2):171–183, 1996.

[7] B. Goyeau, D. Lhuillier, D. Gobin, and M. G. Velarde, "Momentum transport at a fluid–porous interface," *International Journal of Heat and Mass Transfer*, 46(21):4071–4081, 2003.

[8] D. Gobin, B. Goyeau, and A. Neculae, "Convective heat and solute transfer in partially porous cavities," *International Journal of Heat and Mass Transfer*, 48(10):1898–1908, 2005.

[9] M. Prat, "Modelling of heat transfer by conduction in a transition region between a porous medium and an external fluid," *Transport in porous media*, 5(1):71–95, 1990.

[10] J. Alberto O. Tapia and S. Whitaker, "Heat transfer at the boundary between a porous medium and a homogeneous fluid," *International Journal of Heat and Mass Transfer*, 40(11):2691–2707, 1997.

[11] O. M. Haddad, "Fully developed free convection in open-ended vertical channels partially filled with porous material," *Journal of Porous Media*, 2(2), 1999.

[12] A. dHueppe, M. Chandesris, D. Jamet, and B. Goyeau, "Boundary conditions at a fluid–porous interface for a convective heat transfer problem: Analysis of the jump relations," *International Journal of Heat and Mass Transfer*, 54(15):3683–3693, 2011.

[13] S. A. Khashan, A. M. Al-Amiri, and M. A. Al-Nimr, "Assessment of the local thermal non-equilibrium condition in developing forced convection flows through fluid-saturated porous tubes," *Applied thermal engineering*, 25(10):1429–1445, 2005.

[14] P. Forooghi, M. Abkar, and M. Saffar-Avval, "Steady and unsteady heat transfer in a channel partially filled with porous media under thermal non-equilibrium condition," *Transport in porous media*, 86(1):177–198, 2011.

[15] A. dHueppe, M. Chandesris, D. Jamet, and B. Goyeau, "Coupling a two-temperature model and a one-temperature model at a fluid-porous interface," *International Journal of Heat and Mass Transfer*, 55(9): 2510–2523, 2012.

[16] M. Mharzi, M. Daguenet, and S. Daoudi, "Thermosolutal natural convection in a vertically layered fluid-porous medium heated from the side," *Energy conversion and management*, 41(10):1065–1090, 2000.

[17] S. B. Sathe, W. Q. Lin, and T. W. Tong, "Natural convection in enclosures containing an insulation with a permeable fluid-porous interface," *International journal of heat and fluid flow*, 9(4):389–395, 1988.

[18] A. Baytas and I. Pop, "Free convection in a square porous cavity using a thermal nonequilibrium model," *International Journal of Thermal Sciences*, 41(9):861–870, 2002.